

Explaining the mechanism of random lasing based sensing

Michele Gaio,^{1,*} Soraya Caixeiro,¹ Benedetto Marelli,^{2,†} Fiorenzo Omenetto,² and Riccardo Sapienza¹

¹*Department of Physics, King's College London, Strand, London WCR 2LS, United Kingdom.*

²*Department of Biomedical Engineering Tufts University 4 Colby Street, Medford, MA 02155, USA*

(Dated: September 19, 2018)

Here we report a random lasing based sensor which shows pH sensitivity exceeding by 2-orders of magnitude that of a conventional fluorescence sensor. We explain the sensing mechanism as related to gain modifications and lasing threshold nonlinearities. A dispersive diffusive lasing theory matches well the experimental results, and allow us to predict the optimal sensing conditions and a maximal sensitivity as large as 200 times that of an identical fluorescence-based sensor. The simplicity of operation and high sensitivity make it promising for future biosensing applications.

Fluorescence based sensing exploiting spontaneous emission is among the most widespread mechanism for biochemical detection [1, 2]. Latest developments have focussed on improving the biochemistry of the fluorescent binder [3] and on expanding the monitored functionalities [4], as well as on engineering nanoscale light fields via surface plasmons [5], microcavities [6], photonic crystals [7] or optical resonators [8] to enhance light-matter interaction.

Lasing instead, which is based on stimulated emission, has been largely overlooked as a sensing transducer, mainly because of the complexity of a conventional lasing architecture. Lasing has the potential to outperform fluorescence due to the signal amplification inherent to the lasing process, increased signal-to-noise ratio, narrow emission line, and non-linear dynamics, as it has been shown for laser-based interleukin sensing [9], explosives detection [10], and remote identification of hazardous chemicals [11]. Only recently biocompatible lasing architectures made with vitamin [12], and proteins [13, 14] have been fabricated, indicating a path for laser-based biosensing inside living tissues [15].

While conventional lasing requires periodic geometries or carefully aligned cavities, random lasing (RL) occurs in disordered systems with optical gain [16] ranging from semiconductor powers [17, 18] to biomaterials such as human tissue [19]. The lack of an optical cavity gives this structure resilience against deformation and makes it appealing for implantation in biological media. Despite the inherent randomness of RL, emission control has been achieved both spectrally [20, 21] and directionally [22], and its rich modal properties have just started to be explored [23, 24].

Sensing with RL has been limited so far to the detection of changes of the scattering strength of the matrix by a refractive index [19, 25] or temperature [26] variation. Instead, the potential of targeted sensing via biochemical interaction at the gain level, affecting the amplification process, is largely unexplored.

We have recently demonstrated a bio-compatible random laser [14], reacting to pH changes which provides a preliminary sensing proof. In this letter we explain the

mechanism of sensing by random lasing based on gain variation upon interaction with the biochemical environment: the lasing action at neutral pH (Fig. 1(a)), is suppressed at alkaline pH (Fig. 1(b)). The experiments are in very good agreement with the calculations of a dispersive diffusive lasing model without free parameters. We predict the optimal sensing conditions and we show that the random lasing sensitivity can be up to 200 times that of fluorescence.

The random lasing system is fabricated by self-assembly of an inverse silk photonic glass [27] with embedded laser dye (Rhodamine-6G) as detailed in Ref. [14]. The pores have a diameter of $\sim 1.3 \mu\text{m}$ which optimizes the optical scattering (the measured transport mean free path in water is $\ell_t \simeq 14 \mu\text{m}$). The sample (thickness $L \simeq 100 \mu\text{m}$) is excited at a fixed power $P = 840 \mu\text{J}/\text{mm}^2$ with 6 ns pulses of a Nd:YAG Q-switched (wavelength 532 nm, spot diameter $\sim 2 \text{ mm}$) well above the lasing

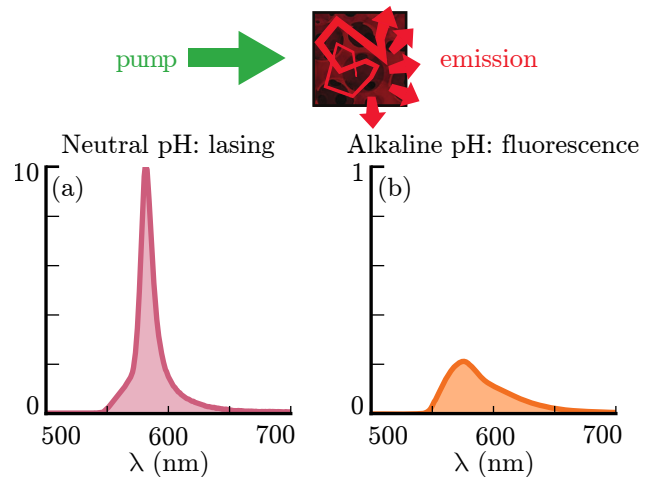


FIG. 1. Random lasing sensing scheme. Light multiple scattering in the gain medium embedded in a photonic glass leads to amplification and lasing. This is experimentally visible in the emission spectrum which shows a narrow band emission (red line, panel (a)). For alkaline pH the lasing emission is switched off resulting in the broadband fluorescence emission and lower intensity (orange line, panel (b)).

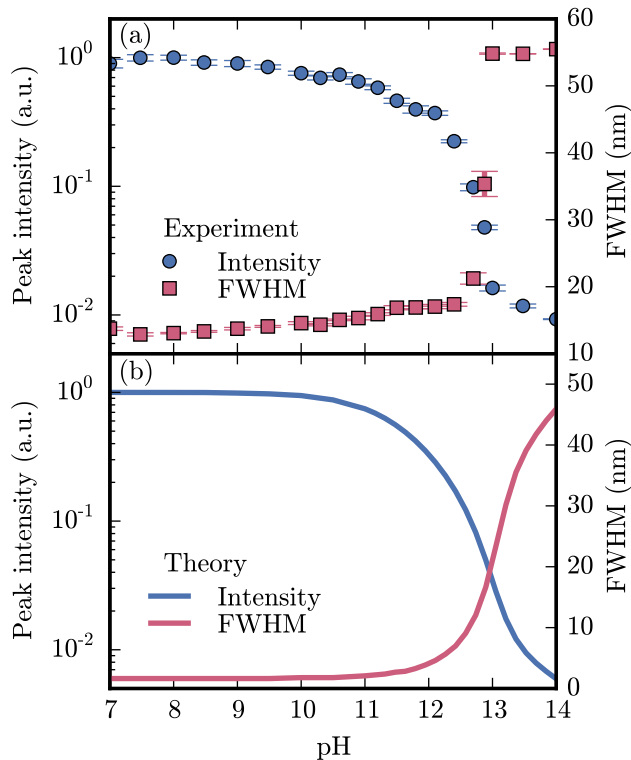


FIG. 2. Sensing of pH: comparison of experiments and theory. (a) The random lasing system is pumped above the lasing threshold ($P = 840 \mu\text{J}/\text{mm}^2$) and the emission characteristics as a function of the pH of the solution are recorded. The lasing is suppressed at large pH values ($\text{pH} > 13$), corresponding to a strong decrease of the peak intensity (blue circles) and a sharp increase of the FWHM of the emission (red square). (b) Theoretical prediction of the lasing response upon pH variation which shows a similar behaviour.

threshold ($T \simeq 80 \mu\text{J}/\text{mm}^2$). The pH of the solution surrounding the laser is controlled by varying the concentration of NaOH. As shown in Fig. 2(a), a progressive decrease in peak intensity (blue circles) is observed for increasing pH: beyond the value $\text{pH} = 13$, the lasing action is switched off. The peak intensity shows an overall ~ 100 -fold intensity decrease, and the full width at half maximum (FWHM) (red squares) instead increases smoothly from 14 nm at $\text{pH} = 7$, corresponding to the above-threshold linewidth (shown in Fig. 1(a)), to $\text{pH} \simeq 13$ where it sharply reaches 54 nm, which is the FWHM of the fluorescence spectrum (shown in Fig. 1(b)). The error bars are calculated as the standard deviation of the average of 10 repeated measurements, each by pumping with a single laser pulse.

This sensing dynamics can be predicted by a dispersive diffusive lasing model, built on light diffusion coupled to classical molecular rate equations and which includes spectral mode competition [28]. This model has no free parameters, it describes the realistic sample char-

acteristics given the scattering and gain properties of the medium either measured or taken from literature [14, 29], while the gain cross-section (σ_e) is calculated by assuming the same scaling of the absorption (σ_a) [29]. The resulting theoretical predictions are shown in Fig. 2(b) and are in very good agreement with the experimental data. As expected [28], the predicted lasing linewidth is underestimated, as in the model the narrowing is limited only by the gain saturation.

Qualitatively, we can understand the lasing switching-off as due to a reduction of the optical amplification which increases the gain length l_g (the distance required for amplification of a factor e): when the critical lasing size $L_{cr} \propto \sqrt{l_t l_g}$ required for lasing becomes larger than the sample size, the lasers switches off. Here the transport mean free path l_t is unchanged by pH variations, whereas the gain length l_g is instead pH sensitive. More quantitatively, in the approximation of a stationary and uniform system, the lasing threshold T can be expressed as

$$T \propto [(N\tau_c v \sigma_e - 1)\tau_r \Phi \sigma_a]^{-1}, \quad (1)$$

where N is the molecules density, v the speed of light in the medium, τ_c is the Thouless time (the typical time it takes for a photon to escape the disordered medium) which accounts for the losses at the surface, and the relevant properties of the molecules providing optical gain are modelled with the stimulated emission cross-section σ_e , the absorption cross section σ_a at the pump wavelength, the radiative lifetime of the excited state τ_r , and the quantum efficiency Φ . The latter two are related via the non radiative decay rate $\Gamma_{nr} = 1/\tau_{nr}$, as $\Phi = \Gamma_r / (\Gamma_r + \Gamma_{nr})$.

A change in any of the molecular parameters in Eq. 1 would modify the lasing threshold and be detectable by the lasing sensor. The dye fluorescence parameters measured as a function of pH, which are the input of the lasing model, are shown in Fig. 3. The dye properties are unaffected in the pH range 7–10. Starting at $\text{pH} \simeq 10$, we observe a pronounced decrease of absorption and lifetime, and from $\text{pH} \simeq 11$ a similar decrease of the quantum efficiency. The quantum efficiency and lifetime are obtained from fluorescence studies of the porous and doped silk matrix with picosecond pulsed excitation ($\lambda = 532 \text{ nm}$, 40 MHz): Φ is obtained as the variation of the fluorescence intensity when recording the light escaping from the sample with an integrating sphere, and τ by fluorescence lifetime spectroscopy by time correlated single photon counting. The absorption is measured with a spectrophotometer and is consistent with lifetime and quantum efficiency as calculated by the Strickler-Berg relation [30]. No significant emission spectral shift is observed. It is evident when comparing Fig. 3 and Fig. 2 that the changes in the molecular properties are amplified by the lasing system and this results in a large intensity variation with a sharp transition of the lasing emission: this offers opportunity for efficient sensing.

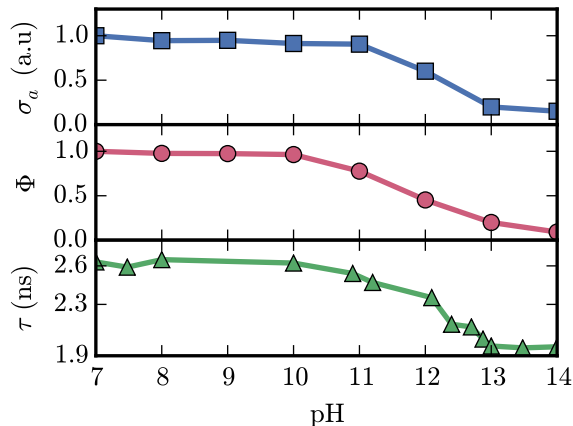


FIG. 3. Rhodamine-6G properties as a function of pH. The relative absorption cross-section (σ_a), quantum efficiency (Φ) and excited state lifetimes (τ) measured as a function of pH. All quantities decrease for pH values larger than $\simeq 10$.

The sensitivity capabilities and limits of RL sensing can be predicted by calculating the effect of the dye parameters on the lasing threshold. Although these parameters are typically coupled in real dyes, we consider them independently to isolate their role. We have chosen as figure of merit the peak intensity (I) relative sensitivity, defined as:

$$S_\alpha = \left| \frac{dI/I}{d\alpha/\alpha} \right|, \quad (2)$$

where α is the parameter examined. The linear response typical of the fluorescence regime would give $S_\alpha = 1$. In Fig. 4 we compute S_α for the various molecular parameters ($\alpha = \sigma_a, \tau, \Phi, \sigma_e$) at different pump intensities. The colormap highlights regions with linear response (white) and highly nonlinear response above $S_\alpha = 1$ (red). The blue areas correspond to regions with little or negligible effect on the measured intensity. The black dashed lines are the calculated lasing threshold, marking the boundary between the fluorescence and lasing regimes. For all parameters there are regions with increased sensitivity when compared to fluorescence ($S_\alpha > 1$).

Fig. 4 can be understood by considering the role of the different molecular parameters in the lasing process. σ_a describes the pump absorption and therefore the excitation probability of the fluorophores. This is a typical property exploited in fluorescence sensing as it induces a variation of the measured emitted light intensity. In the regime where RL has sizes exceeding the penetration depth of the pump, a change in pump absorption can be compensated by an increase of the active volume inside the system, such that the total available gain is the same, *i.e.* for large absorption values (right side of Fig. 4(a)) the RL is insensitive to changes in σ_a . Instead, for lower absorption values (left side of Fig. 4(a)), when the pump

absorption length is comparable with the system size, the absorbed intensity and the emission intensity are linearly related to σ_a both for fluorescence and lasing (white areas). Interestingly, around the lasing threshold (the black line), a twofold increase in the sensitivity $S_{\sigma_a} = 2.2$ (light red region) is predicted.

A similar behaviour can be observed for τ which instead describes the lifetime of the population of the excited state and therefore is related to the ease of inducing population inversion. As shown in Fig. 4(b), the recorded intensity is largely insensitive to a change of τ , both for fluorescence and lasing. Instead, a lifetime decrease induces a mild shift of the lasing threshold towards higher pump intensities resulting in a roughly linear sensitivity, with $S_\tau = 0.9$ around the lasing threshold.

The quantum efficiency Φ is another quantity often exploited in fluorescence sensing techniques, as it relates directly to the emitted intensity. The wide linear (white) region below lasing threshold in Fig. 4(c) is the linear sensitivity of the fluorescence regime. The lasing emission intensity well above threshold is marginally affected by the quantum efficiency, because non-radiative decay processes are slower than stimulated emission and therefore they become irrelevant. Instead, around the lasing threshold the sensitivity peaks, up to $S_\Phi = 201$, as shown by the red region. This can be understood as the emission intensity increases rapidly as stimulated emission (unaffected by Φ) takes over spontaneous emission (affected by Φ).

The most direct way of tuning the lasing threshold is by controlling the gain value, *i.e.* altering σ_e as shown in Fig. 4(d). This is a parameter unique to lasing, which has no effect on fluorescence. As expected, the calculated fluorescence sensitivity is independent from σ_e and once again the largest response is found around the lasing threshold. In this case, a decrease of σ_e to roughly 10% of the original value results in the suppression of the lasing emission, regardless of the pump intensity. In these conditions, high sensitivity ($S_{\sigma_e} = 186$) is reached.

We can now discuss the experimental sensing profile reported in Fig. 2. The top bars in Fig. 4 identify the measured variation of the parameters. As expected a pH variation affects all of them, but most notably the gain and quantum efficiency. The resulting experimental sensitivity extracted from the experimental data is $S_{\text{pH}} = 200 \pm 50$ at pH = 13, which is larger than the theoretical expectation of $S_{\text{pH}} \sim 60$. Finally, in the range pH = 12–13, we estimate a limit of detection (LOD) of $\text{LOD}_{\text{pH}} \simeq 0.03$, defined as 3 times the signal to noise ratio.

Stimulated emission can therefore boost the sensitivity of a fluorescence sensor as well as provide an additional sensing parameter, *i.e.* σ_e . These advantages come at the expense of additional complexity. Lasing requires a nanophotonic architecture to promote stimulated emission, a disordered medium for RL, and a dye capable of

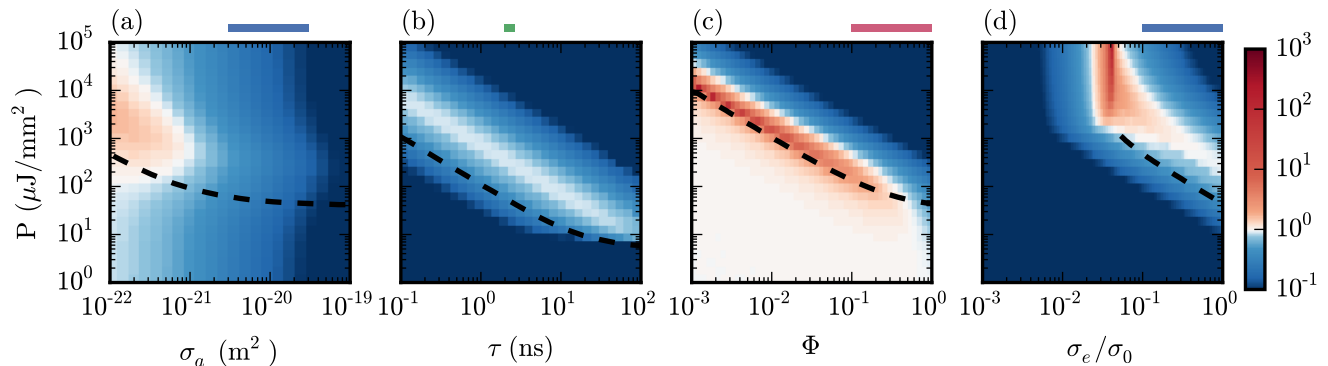


FIG. 4. Sensitivity analysis. The relative sensitivity defined as $S_\alpha = \left| \frac{dI/I}{d\alpha/\alpha} \right|$, for $\alpha = \sigma_a, \tau, \Phi, \sigma_e$, is calculated for the same system parameters, when varying the value of α , and for different pump intensities. The black dashed lines are the lasing threshold marking the boundary between the fluorescence and lasing regime. The blue areas correspond to no-sensitivity ($S_\alpha \ll 1$), the white areas correspond to linear sensitivity ($S_\alpha = 1$), and the red areas correspond to increased sensitivity ($S_\alpha \gg 1$). The highest sensitivities are found around the fluorescence-lasing transition, with maximum values $S_{\sigma_a} = 2.2$, $S_\tau = 0.9$, $S_\Phi = 201$, $S_{\sigma_e} = 186$. The top bars refer to the measured variation of each parameter as shown in Fig. 3.

providing net optical gain. The large $\sim (10 \mu\text{m})^3$ laser volume implies that the RL sensor is not suitable for sensitivity at the single molecule level. When compared to fluorescence schemes, RL requires a higher excitation intensity, in the μW range ($> 1 \mu\text{J}$ pulse energy) instead of the nW range of conventional single molecule spectroscopy. While this could be a problem for in vivo sensing, preliminary results in living cells [31, 32] show that these power ranges are below the damage threshold of the biological media.

In conclusion, we have introduced a RL sensing scheme based on the lasing threshold shift upon modification of the gain dye parameters. We have presented a detailed description of the sensing mechanism and a theoretical model which matches very well the experiments on pH sensing by silk-based random lasing. We have identified the most efficient sensing scheme, with a 2-order of magnitude enhancement with respect to fluorescence. Given the universality of multiple scattering, its robustness against stress and deformation, and the large availability of fluorescent and lasing dyes, we foresee possible applications for bio and chemical sensing in living tissues.

We wish to thank Duong Van Ta and Francisco Fernandes for fruitful discussions. The research leading to these results has received funding from the Engineering and Physical Sciences Research Council (EPSRC), from the European Union, from the Leverhulme Trust and from the Royal Society. F.G.O. would like to acknowledge the Office of Naval Research for support of this work (N00014-13-1-0596).

[†] Present address: Department of Civil and Environmental Engineering MIT, 77 Massachusetts Avenue, Cambridge, MA 02139-4307, USA

- [1] Stephan Schreml, Robert J Meier, Otto S Wolfbeis, Michael Landthaler, Rolf-Markus Szeimies, and Philipp Babilas, “2D luminescence imaging of pH in vivo.” *Proc. Natl. Acad. Sci. U. S. A.* **108**, 2432–2437 (2011).
- [2] Yan Geng, Mohammad A. Ali, Andrew J. Clulow, Shengqiang Fan, Paul L. Burn, Ian R. Gentle, Paul Meredith, and Paul E. Shaw, “Unambiguous detection of nitrated explosive vapours by fluorescence quenching of dendrimer films,” *Nat. Commun.* **6**, 8240 (2015).
- [3] A.P. Demchenko, *Introduction to Fluorescence Sensing*, Biomedical and Life Sciences (Springer Netherlands, 2008).
- [4] Marina K. Kuimova, Stanley W. Botchway, Anthony W. Parker, Milan Balaz, Hazel A. Collins, Harry L. Anderson, Klaus Suhling, and Peter R. Ogilby, “Imaging intracellular viscosity of a single cell during photoinduced cell death,” *Nat. Chem.* **1**, 69–73 (2009).
- [5] Wei Deng and Ewa M. Goldys, “Plasmonic approach to enhanced fluorescence for applications in biotechnology and the life sciences,” *Langmuir* **28**, 10152–10163 (2012).
- [6] F. Vollmer, D. Braun, A. Libchaber, M. Khoshhima, I. Teraoka, and S. Arnold, “Protein detection by optical shift of a resonant microcavity,” *Appl. Phys. Lett.* **80**, 4057–4059 (2002).
- [7] I. V. Soboleva, E. Descrovi, C. Summonte, A. A. Fedyanin, and F. Giorgis, “Fluorescence emission enhanced by surface electromagnetic waves on one-dimensional photonic crystals,” *Appl. Phys. Lett.* **94** (2009), 10.1063/1.3148671.
- [8] Gleb M. Akselrod, Brian J. Walker, William A. Tisdale, Mounji G. Bawendi, and Vladimir Bulovic, “Twenty-fold enhancement of molecular fluorescence by coupling to a J-aggregate critically coupled resonator,” *ACS Nano* **6**, 467–471 (2012).
- [9] Xiang Wu, Maung Kyaw Khaing Oo, Karthik Reddy, Qiushu Chen, Yuze Sun, and Xudong Fan, “Optofluidic laser for dual-mode sensitive biomolecular detection with

* michele.gaio@kcl.ac.uk

- a large dynamic range.” *Nat. Commun.* **5**, 3779 (2014).
- [10] Aimée Rose, Zhengguo Zhu, Conor F Madigan, Timothy M Swager, and Vladimir Bulović, “Sensitivity gains in chemosensing by lasing action in organic polymers.” *Nature* **434**, 876–879 (2005).
- [11] Brett H Hokr, Joel N Bixler, Gary D Noojin, Robert J Thomas, Benjamin a Rockwell, Vladislav V Yakovlev, and Marlan O Scully, “Single-shot stand-off chemical identification of powders using random Raman lasing.” *Proc. Natl. Acad. Sci. U. S. A.* **111**, 12320–4 (2014).
- [12] Sedat Nizamoglu, Malte C. Gather, and Seok Hyun Yun, “All-biomaterial laser using vitamin and biopolymers,” *Adv. Mater.* **25**, 5943–5947 (2013).
- [13] Yunkyong Choi, Heonsu Jeon, and Sunghwan Kim, “A fully biocompatible single-mode distributed feedback laser,” *Lab on a Chip* **15**, 642–645 (2015).
- [14] Soraya Caixeiro, Michele Gaio, Benedetto Marelli, Fiorenzo G. Omenetto, and Riccardo Sapienza, “Silk-Based Biocompatible Random Lasing,” *Adv. Opt. Mater.* **4**, 998–1003 (2016).
- [15] Xudong Fan and Seok-Hyun Yun, “The potential of optofluidic biolasers.” *Nat. Methods* **11**, 141–7 (2014).
- [16] Diederik S. Wiersma, “The physics and applications of random lasers,” *Nat. Phys.* **4**, 359–367 (2008).
- [17] H Cao, Y G Zhao, S T Ho, E W Seelig, Q H Wang, and R P H Chang, “Random laser action in semiconductor powder,” *Phys. Rev. Lett.* **82**, 2278–2281 (1999).
- [18] Karen L. Van Der Molen, R. Willem Tjerkstra, Allard P. Mosk, and Ad Lagendijk, “Spatial extent of random laser modes,” *Phys. Rev. Lett.* **98** (2007), 10.1103/PhysRevLett.98.143901.
- [19] Randal C. Polson and Z. Valy Vardeny, “Random lasing in human tissues,” *Appl. Phys. Lett.* **85**, 1289–1291 (2004).
- [20] Stefano Gottardo, Riccardo Sapienza, Pedro D. García, Alvaro Blanco, Diederik S. Wiersma, and Cefe López, “Resonance-driven random lasing,” *Nat. Photonics* **2**, 429–432 (2008).
- [21] Nicolas Bachelard, Sylvain Gigan, Xavier Noblin, and Patrick Sebbah, “Adaptive pumping for spectral control of random lasers,” *Nature Physics* **10**, 426–431 (2014).
- [22] Thomas Hisch, Matthias Liertzer, Dionyz Pogany, Florian Mintert, and Stefan Rotter, “Pump-Controlled Directional Light Emission from Random Lasers,” *Physical Review Letters* **111**, 023902 (2013).
- [23] F. Antenucci, C. Conti, A. Crisanti, and L. Leuzzi, “General phase diagram of multimodal ordered and disordered lasers in closed and open cavities,” *Phys. Rev. Lett.* **114**, 1–5 (2015).
- [24] Marco Leonetti, Claudio Conti, and Cefe Lopez, “The mode-locking transition of random lasers,” *Nat. Photonics* **5**, 615–617 (2011).
- [25] Seung Ho Choi and Young L. Kim, “The potential of naturally occurring lasing for biological and chemical sensors,” *Biomedical Engineering Letters* **4**, 201–212 (2014).
- [26] D S Wiersma and S Cavalieri, “Light emission: A temperature-tunable random laser.” *Nature* **414**, 708–709 (2001).
- [27] Pedro David García, Riccardo Sapienza, and Cefe López, “Photonic glasses: A step beyond white paint,” *Advanced Materials* **22**, 12–19 (2010).
- [28] Michele Gaio, Matilda Peruzzo, and Riccardo Sapienza, “Tuning random lasing in photonic glasses,” *Opt. Lett.* **40**, 1611–1614 (2015).
- [29] W. Holzer, H. Gratz, T. Schmitt, A. Penzkofer, A. Costela, I. Garca-Moreno, R. Sastre, and F.J. Duarte, “Photo-physical characterization of rhodamine 6G in a 2-hydroxyethyl-methacrylate methyl-methacrylate copolymer,” *Chem. Phys.* **256**, 125–136 (2000).
- [30] S. J. Strickler and Robert a. Berg, “Relationship between Absorption Intensity and Fluorescence Lifetime of Molecules,” *J. Chem. Phys.* **37**, 814 (1962).
- [31] Marcel Schubert, Anja Steude, Philipp Liehm, Nils M. Kronenberg, Markus Karl, Elaine C. Campbell, Simon J. Powis, and Malte C. Gather, “Lasing within Live Cells Containing Intracellular Optical Microresonators for Barcode-Type Cell Tagging and Tracking,” *Nano Letters* **15**, 5647–5652 (2015).
- [32] Matjaž Humar and Seok Hyun Yun, “Intracellular micro-lasers,” *Nature Photonics* **9**, 572–576 (2015).